Fish and Shellfish Immunology 95 (2019) 140–150

Contents lists available at ScienceDirect

Fish and Shellfish Immunology

journal homepage: www.elsevier.com/locate/fsi

Full length article

Characterization and expression analysis of immune-related genes in the red swamp crayfish, *Procambarus clarkii* in response to lipopolysaccharide challenge

Ting Jiao[a,b,1], Ting-Ting Yang[a,c,e,1], Dong Wang[f], Zhen-Qiu Gao[a,d], Jia-Lian Wang[a], Bo-Ping Tang[a], Qiu-Ning Liu[a,c,*], Dai-Zhen Zhang[a,**], Li-Shang Dai[b,***]

[a] Jiangsu Key Laboratory for Bioresources of Saline Soils, Jiangsu Synthetic Innovation Center for Coastal Bio-agriculture, Jiangsu Provincial Key Laboratory of Coastal Wetland Bioresources and Environmental Protection, School of Ocean and Biological Engineering, Yancheng Teachers University, Yancheng, 224007, PR China
[b] School of Pharmaceutical Sciences, Wenzhou Medical University, Wenzhou, 325035, PR China
[c] Key Laboratory of Insect Developmental and Evolutionary Biology, CAS Center for Excellence in Molecular Plant Sciences, Shanghai Institute of Plant Physiology and Ecology, Chinese Academy of Sciences, Shanghai, 200032, PR China
[d] School of Pharmacy, Yancheng Teachers University, Yancheng, 224007, PR China
[e] College of Biotechnology and Pharmaceutical Engineering, Nanjing University of Technology, Nanjing, 210009, PR China
[f] Instrumental Analysis Center, Yancheng Teachers University, Yancheng, 224007, PR China

ARTICLE INFO

Keywords:
Immune-related genes
Lipopolysaccharide
Procambarus clarkii

ABSTRACT

To learn more about red swamp crayfish related genes in response to bacterial infections, we investigated immune-related genes induced by lipopolysaccharide (LPS) in the hepatopancreas using high-throughput sequencing method. In present the study, a total of 55,107 unigenes were identified, with an average length of 678 bp. A total of 2215 differentially expressed genes (DEGs) were found, including 669 up-regulated genes and 1546 down-regulated genes. The result of Gene ontology (GO) analysis revealed that 3017 DEGs were enriched in 19 biological process subcategories, 17 cellular component subcategories and 15 molecular function subcategories. The top 20 Kyoto Encyclopedia of Genes and Genomes (KEGG) pathways showed that "ribosome" was the most abundant group, which had 34 DEGs. KEGG enrichment analysis identified several immune response pathways. Real-time quantitative reverse transcription-PCR (qRT-PCR) results exhibited that several immune responsive genes were greatly up-regulated following LPS stimulation as observed in the results of high-throughput sequencing. Overall, this study provides new insight into the immune defense mechanisms of *P. clarkii* against LPS infection.

1. Introduction

The red swamp crayfish, *Procambarus clarkii*, is distributed in the natural eco-environment worldwide, because of its strongly adaptive ability and high fecundity [1]. *P. clarkii* is an important source of high nutritional proteins, which contains all the essential amino acids required for human nutrition [2]. Owning to its rapid growth rate and high economic value, *P. clarkii* farming is becoming a rapidly developing aquaculture industry in China, particularly in Jiangsu province [3–5]. *P. clarkii* has also been artificially cultivated because of their superior disease resistance against pathogens [6]. Furthermore, it has frequently been used as a model organism to study the molecular mechanisms of invertebrate innate immunity [7]. The global shrimp industry still faces different serious disease-related problems that are mainly caused by pathogenic bacteria and viruses [8], such as WSSV [9], IHHNV [10], *Vibrio alginolyticus* [11], and *Spiroplasma eriocheiris* [12]. Therefore, the knowledge on the immune system of crayfish is highly important for diseases management and development of sustainable crayfish culture [13].

So far, only few studies reported the immune response of shrimp [14]. We selected the hepatopancreas as a target tissue. As an integrated organ of immunity and metabolism, hepatopancreas as an

* Corresponding author. School of Pharmaceutical Sciences, Wenzhou Medical University, Wenzhou, 325035, PR China.
** Corresponding author. School of Pharmaceutical Sciences, Wenzhou Medical University, Wenzhou, 325035, PR China.
*** Corresponding author.
E-mail addresses: liuqn@yctu.edu.cn (Q.-N. Liu), zhangdz@yctu.edu.cn (D.-Z. Zhang), lishang2016@wmu.edu.cn (L.-S. Dai).
[1] These authors contributed equally to this work.

https://doi.org/10.1016/j.fsi.2019.09.072
Received 7 August 2019; Received in revised form 27 September 2019; Accepted 30 September 2019
Available online 16 October 2019

Table 1
Primers used for qRT-PCR.

Primer name	Forward Primer (5′-3′)	Reverse Primer (5′-3′)	Purpose
Cofilin	ATGGCATCTGGAGTGAAAGT	TGCTCAGGTGCTGTAGGTAAT	qRT-PCR
Cysteine proteinase	AAGTATGTTGACGCAGAGGAGG	AAATTGGTTCATTGCCAGGTTG	qRT-PCR
HSP21	TTCAGCCGTCGCTTCAATCT	AGAGCTTTTGGACGCCTTGA	qRT-PCR
HSP70	CCTTCACCGACACAGAACGA	ACCGATGAGTCGTTTGGCAT	qRT-PCR
Phospholipase D	TCTCTTTCCCCTCCCGCCACAAC	ACTCACGCTCCACCCAACAATG	qRT-PCR
Myeloid differentiation factor 88	CGCCGACGCATTGTCATTC	TGCTCGTGGTTCACTGGAT	qRT-PCR
Ras-related protein Ral-a	GATGTCCGGCGCCAAGAAAAAC	TCCTGTCCTGCCGTGTCAAGAAT	qRT-PCR
Serine/threonine protein kinase	TGCTATGTGAAGCTCGGCTCT	GCGATCTGATGCTCCTCCTCT	qRT-PCR
TGF beta-inducible nuclear protein	GCCTGGGTGCTGGTATCTTGG	GTTCGTTCTGTGGCATTGTGT	qRT-PCR
Tar RNA binding protein	AAAATGTATCGTCAACCACCAC	CACCCTCTATCTGCAACAAGTC	qRT-PCR
18S	ACCGATTGAATGATTTAGTGAG	TACGGAAACCTTGTTACGAC	qRT-PCR

Table 2
Quality of clean reads.

Samples	Clean reads	Clean bases	GC content	% > =Q30	Mapped reads	Unique mapped reads	Multi mapped reads
PBS	22,067,581	6,589,701,420	53.79%	92.37%	16,817,240 (76.21%)	8,589,918 (51.08%)	8,227,322 (48.92%)
LPS	31,305,267	9,371,998,450	49.07%	92.41%	24,022,870 (76.74%)	15,257,941 (63.51%)	8,764,929 (36.49%)

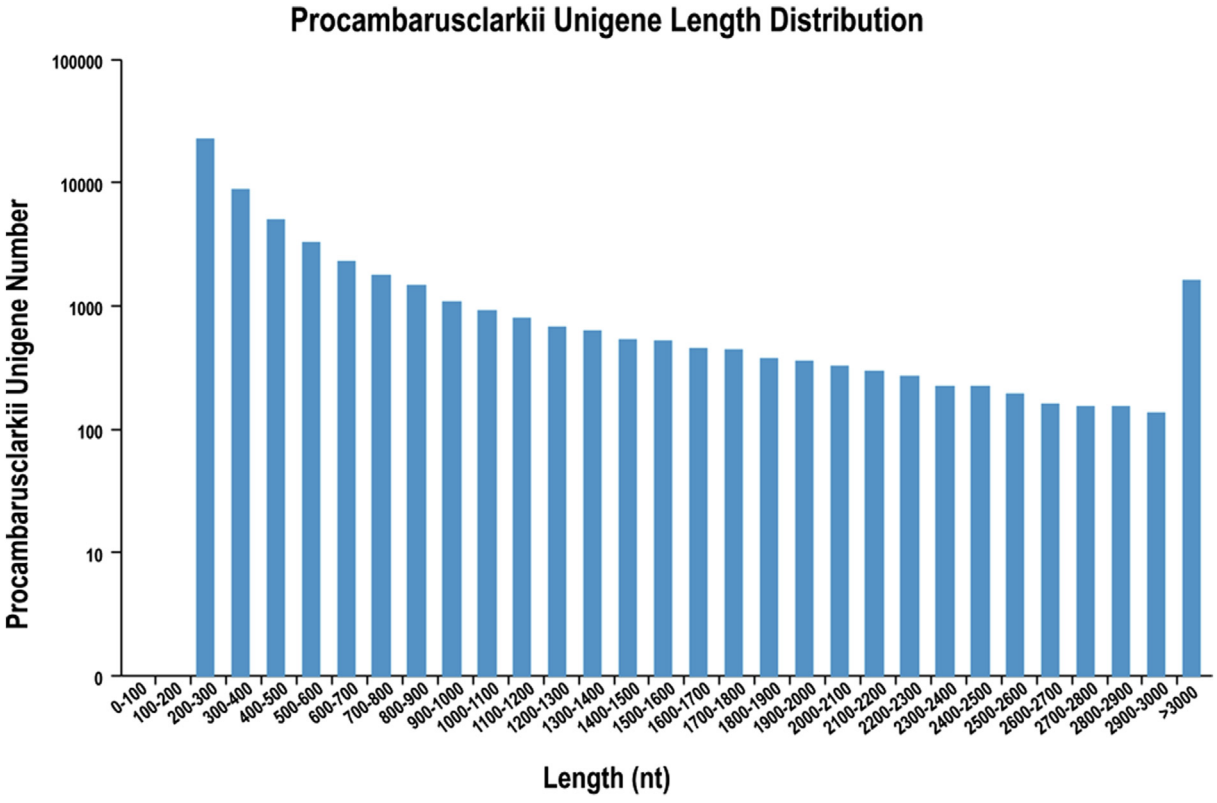

Fig. 1. The length distribution of the unigenes in the *P. clarkii* hepatopancreas transcriptome.

Table 3
Distribution of splicing length.

Length range	Transcript	Unigene
200–300	25,653 (32.66%)	22,432 (40,71%)
300–500	17,388 (22.14%)	13,575 (24.63%)
500–1000	15,140 (19.28%)	9800 (17.78%)
1000–2000	10,985 (13.99%)	5609 (10.18%)
2000 +	9376 (11.94%)	3691 (6.70%)
total number	78,542	55,107
total length	73,001,954	37,373,065
N50 length	1805	1136
Mean length	929.46	678.19

important organ plays a key role in immune response during acute virus infection and infection-induced metabolic changes [15]. Crustacean hepatopancreas also has multiple biological functions such as secreting immune digestive enzymes, detoxification of toxic materials, regulates metabolic processes, biogenesis and innate immune processes. It is worth noting that crustacean hepatopancreas is particularly susceptible to infections, and many diseases can be diagnosed by evidence of hepatopancreas pathology or by its physiological state [16]. Thus, the knowledge on its immune genes is crucial to understand antimicrobial mechanisms [17]. The crustacean immune system is mainly based on innate immune defense [18]. The innate immune system is made up of a variety of physical barriers, chemical and cellular components that

Table 4
Summary statistics of the *P. clarkii* transcriptome annotation.

Annotated databases	Annotated number	Percentage (%)	300 ≤ Length < 1000	Length ≥ 1000
COG_annotation	5712	31.10	1839	2425
GO_annotation	7683	41.83	2802	2777
KEGG_annotation	8534	52.11	2956	3634
KOG_annotation	12,527	46.46	4233	4950
Pfam_annotation	12,958	70.55	4460	5563
Swissprot_annotation	9298	50.62	3136	4141
EggNOG_annotation	16,898	92.00	5890	5975
NR_annotation	15,551	84.67	5790	6128
All_annotated	18,367	100	6572	6261

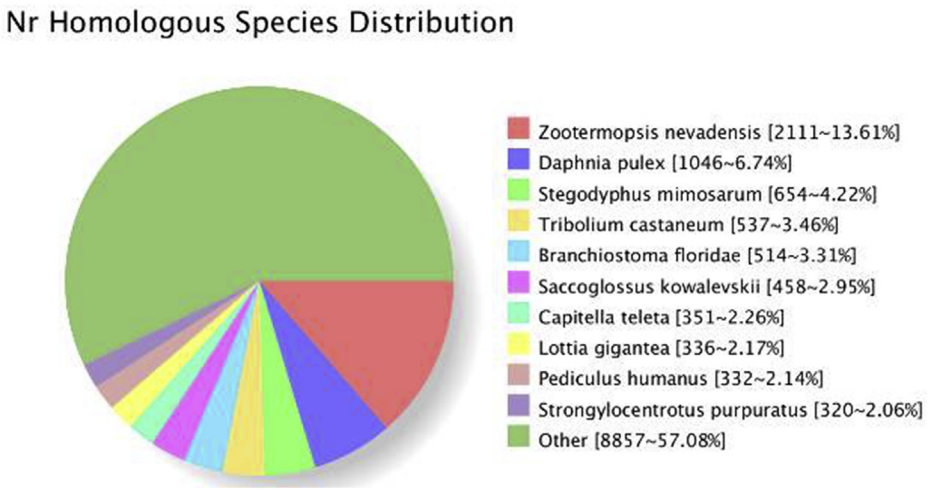

Fig. 2. Comparison of *P. clarkii* hepatopancreas transcriptomic sequences with the known sequences in databases.

form the first line of defense for the body against foreign antigens and invading pathogens before they establish full infection in cells [19,20]. The invertebrate immune system must rely on non-self-recognition molecules to ensure efficient defense responses against infectious pathogens that continuously threaten their survival. Lipopolysaccharide (LPS) from bacterial endotoxin has been regarded as a potential molecule involved in immune recognition and immune defense, and it is the major constituent of the outer membrane of all Gram-negative bacteria [21]. This reveals that the release of LPS from bacteria into bloodstream may cause serious unwanted stimulation of the host immune system [22].

In the present study, two transcriptome sequencing libraries were constructed with the hepatopancreas of *P. clarkii* from LPS infection group and Phosphate buffer saline (PBS) group. High-throughput sequencing was carried out to do a comparative analysis. RNA-sequencing (RNA-seq) provides a revolutionary way to unveil transcription by using ultra-high-throughput sequencing technologies to generate hundred millions of short reads from RNA molecules [23]. Differentially expressed genes (DEGs) were analyzed and identified by comparing two libraries using different functional databases. Subsequently, we performed Gene Ontology (GO) enrichment and Kyoto Encyclopedia of Genes and Genomes (KEGG) enrichment analysis to enrich these DEGs and identified the immune-related DEGs. Taken together, our study will shed a new light on the immune system and defense mechanisms of *P. clarkii*, and pave a new way for fighting against LPS stimulation in *P. clarkii*.

2. Materials and methods

2.1. Experimental P. clarkii preparation and immune challenge

P. clarkii with average body weight of 15 g and length of 8–9 cm were purchased from a farming pond in Yancheng, Jiangsu Province, China. Then, we cultured them at 24 °C in water for several weeks. The individuals were divided into two groups: LPS group and PBS group. Three samples were chosen to be injected with 10 μl LPS (0.001 g/ml) and were regarded as testers. At the same time, three samples were injected with 10 μl PBS, which were served as controls. In our study, the hepatopancreas of six crayfish in two groups after 24 h infection was collected for research and these samples were kept at −80 °C.

2.2. RNA extraction, cDNA library construction and transcriptome sequencying

Total RNA was separately extracted using Trizol (Sangon, China) and treated with RNase-free DNase (Promega, China), according to the manufacturer's instructions. RNA purity was assessed by the NanoPhotometer spectrophotometer (Implen, USA). The RNA Nano 6000 Assay Kit and the Agilent Bioanalyzer 2100 system (Agilent Technologies, USA) were used to evaluate the RNA integrity. In addition, RNA concentration was determined using the Qubit RNA Assay Kit in a Qubit 2.0 Fluorometer (Life Technologies, CA, USA).

cDNA libraries were prepared using TruSeq RNA Sample Prep Kit (Illumina) [24]. Briefly, the mRNA was purified with poly-T magnetic beads and then fragmented and reverse transcribed into double-stranded cDNA. mRNA was randomly interrupted by Fragmentation Buffer. First strand cDNA was synthesized using a random hexamer primer and M-MLV Reverse Transcriptase. RNase H and DNA polymerase I were used to perform second strand cDNA synthesis subsequently. The remaining overhangs were converted into blunt ends via exonuclease/polymerase activities. After adenylation of the 3′ ends of DNA fragments, NEBNext Adaptors with hairpin loop structures were ligated to prepare for hybridization. cDNA was purified with the AMPure XP beads. The purified double-stranded cDNA was subjected to

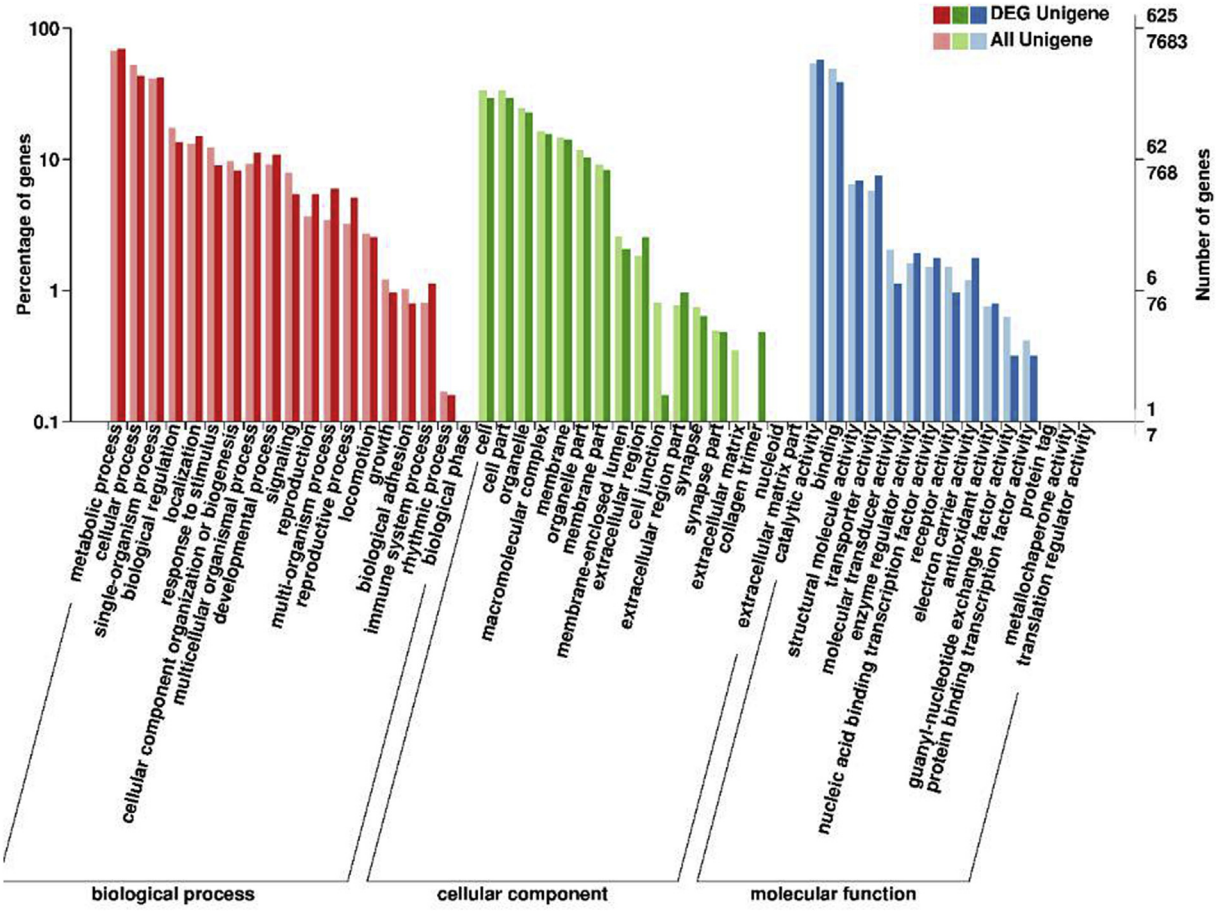

Fig. 3. Histogram description of Gene Ontology enrichment of DEGs. All the DEGs fell into three categories: cellular component (CC), molecular function (MF), and biological process (BP). The X-axis represents various gene function, and Y-axis corresponds to the number of DEGs.

terminal repair and then ligated to sequencing adapters. The sequencing depth was 6G and the length of Illumina sequencing was 37,373,065 bp.

2.3. De novo assembly of sequencing reads

The files from all libraries on the left file (read1 files) were pooled into one big left. fq file, and right files (read2 files) into one big right. fq file [25]. After cleaning and filtering out linker sequence and low-quality reads from the raw data, the remaining high quality clean reads were *de novo* assembled by Trinity software [26]. Meanwhile, Q20, Q30, GC-content and sequence duplication level of the clean reads were measured. Low-quality reads were discarded by setting the maximum expected error threshold (E_max), which is the sum of the error probability provided by the Q score for each base, to 1.

2.4. Transcriptome annotation and classification

Gene function was annotated based on the following databases: NCBI non-redundant protein sequences (NR) (ftp://ftp.ncbi.nih.gov/blast/db/) [27]; NCBI non-redundant nucleotide sequences (NT) (ftp://ftp.ncbi.nih.gov/blast/db/FASTA/); Protein family (Pfam) (http://pfam.xfam.org/); Clusters of Orthologous Groups of proteins (KOG/COG) (http://www.ncbi.nlm.nih.gov/KOG; http://www.ncbi.nlm.nih.gov/COG/) [28]; Swiss-Prot (http://www.uniprot.org/downloads) [29]; KEGG (http://www.genome.jp/kegg) [30]; and GO (http://www.geneontology.org/) [31]. Among these databases, COG is a valuable resource that allows more accurate and reliable functional prediction and classification of gene products based on their orthologous relationship [32]. All unigenes were used as queries in searching NR, Swiss-Prot and functionally annotated by GO analysis with Blast2GO software (http://www.blast2go.org/) [33]. Blast2GO and WEGO software were applied to assign GO annotations and perform GO function classification analysis for the unigenes [34].

2.5. Differentially expressed genes and enrichment analysis

The expression level of overall unigenes was normalized to determine FPKM (Fragments per kilobase of exon model per million mapped fragments) using RSEM [35]. The gene expression levels were measured by mapping the clean reads of each sample to the Trinity transcript assembly through RSEM software [36]. Differential expression analysis was performed of the different libraries using the DESeq R package [37]. Based on the negative binomial distribution model, the DESeq software conducts normalizations, variance estimations, and differential expression of raw read counts and works best with experiments that have replicates [38]. The resulting *P*-values were adjusted for controlling the false discovery rate (FDR). Genes with an adjusted *P*-value < 0.05 checked by DESeq were assigned as differentially expressed. Significance of DEGs ($(|\log2(\text{foldchange})|) \geq 2$, FDR < 0.01) were identified between LPS and PBS group. Then, GO enrichment and KEGG enrichment analysis were used to enrich DEGs for further study. The functional enrichment analysis is a comparative analytical method that is used to identify enriched genes in the datasets of interest for molecular functions, biological processes and pathways. GO annotation has been broadly utilized as functional enrichment studies for large-scale genes [39]. GO enables gene to be classified and grouped together according to their functional properties, and describes the attributes of

Table 5
Table of GO enrichment of all genes and DEGs.

Subcategories	Term type	Unigenes	DEGs
Metabolic process	Biological process (BP)	3893	318
Cellular process		3992	264
Single-organism process		2948	232
Biological regulation		1294	80
Localization		957	84
Response to stimulus		1053	58
Cellular component organization or biogenesis		778	53
Multicellular organismal process		734	74
Developmental process		713	69
Signaling		726	36
Reproduction		287	35
Multi-organism process		274	39
Reproductive process		253	33
Locomotion		218	16
Growth		202	11
Biological adhesion		87	6
Immune system process		81	9
Rhythmic process		17	1
Biological phase		3	0
Cell	Cellular component (CC)	2570	182
Cell part		2568	182
Organelle		1899	141
Macromolecular complex		1250	97
Membrane		1122	89
Organelle part		907	65
Membrane part		699	52
Membrane-enclosed lumen		200	13
Extracellular region		140	16
Cell junction		62	1
Extracellular region part		59	6
Synapse		57	4
Synapse part		38	3
Extracellular matrix		27	0
Collagen trimer		4	3
Nucleoid		3	0
Extracellular matrix part		3	0
Catalytic activity	Molecular function (MF)	4179	357
Binding		3785	242
Structural molecule activity		497	43
Transporter activity		446	47
Molecular transducer activity		158	7
Enzyme regulator activity		124	12
Nucleic acid binding transcription factor activity		116	11
Receptor activity		116	6
Electron carrier activity		92	11
Antioxidant activity		58	5
Guanyl-nucleotide exchange factor activity		48	2
Protein binding transcription factor activity		32	2
Protein tag		2	0
Metallochaperone activity		1	0
Translation regulator activity		1	0

genes and gene products in organisms [40]. The KEGG database acts as a major knowledgebase and one of the most authoritative biological databases in the world to provide significant details regarding the biological pathways and molecular networks associated with the given genes and transcripts [41].

2.6. qRT-PCR of genes expression

To further identify the expression levels of immune-related genes, we used qRT-PCR to confirm our sequencing results. cDNA template was synthesized by the TUREscript cDNA Synthesize Kit (Aidlab, China). The 18S rRNA gene was used as a reference gene [18,42]. Then, qRT-PCR specific primers were designed using Primer Premier 5.0 software (Table 1). The qPCR reactions were carried out in a 20 μl volume containing 10 μl of 2 × SYBR Green qPCR Mix, 1 μl of forward and reverse primers, 1 μl of cDNA template, and 7 μl of RNase-free H_2O. The amplification circumstance was as follows: 95 °C for 10 s, followed by 40 cycles of 95 °C for 15 s, 55 °C for 15 s, and 72 °C for 30 s. The final concentration of the primer was 0.5 mM/μl. The gene expression level changes were determined using the $2^{-\Delta\Delta CT}$ method [43]. Data are presented as the mean ± standard error of the mean, the SPSS 16.0 program (SPSS, USA) was used to Statistical analysis. The data were subjected to a one-way analysis of variance (ANOVA), followed by Duncan's Multiple Range test, and the values were significantly different to the control at the same time point when marked with asterisks (*$P < 0.05$, **$P < 0.01$, ***$P < 0.001$).

3. Results and discussion

3.1. De novo assembly and splicing

We used Illumina Hiseq 2000 sequencing platform to construct cDNA libraries of experimental and control groups. A total of 22,067,581 clean reads from PBS-injected group and 31,305,267 clean reads from LPS-challenged group were obtained. There were 6,589,701,420 clean bases in PBS group while LPS group has 9,371,998,450 clean bases. Q30 was higher than 92%, and the G + C content was approximately 54% in PBS-injected samples and 49% in LPS-treated samples. Besides, 16,817,240 (76.21%) and 24,022,870 (76.74%) clean reads were respectively obtained from two groups. The results revealed that 15,257,941 (63.51%) of the reads were uniquely mapped to the genome for the LPS group and 8,589,918 (51.08%) for the control group. Furthermore, 8,764,929 (36.49%) and 8,227,322 (48.92%) of the reads, respectively, were multiply mapped to these groups (Table 2). Using Trinity v2.0.6, 78,542 transcripts were generated with mean length of 929.46 bp and N50 length of 1805 bp; 55,107 unigenes were identified with average length of 678.19 bp and N50 length of 1136 bp.The results also exhibited that most of the unigenes were distributed at 200–300 bp, 300–500 bp, and 500–1000 bp. Among these unigenes, 36,007 (65.34%) were within the range of 200–500 bp, 9800 (17.78%) were 500–1000 bp, 5609 (10.18%) were 1–2 kbp, and 3691 (6.70%) unigenes were longer than 2kbp (Fig. 1 and Table 3). These results indicate that the data is of high-quality, and the obtained unigenes are reliable and suitable for annotation analysis.

3.2. Functional annotation of assembled unigenes

To further understand the molecular functions of the genes, we annotated the unigenes against seven databases, including NR, Swiss-Prot, GO, COG, KOG, eggNOG, and KEGG. The number of unigenes that could be annotated in the different databases were as follows: 15,551 in NR (84.67%); 8534 in KEGG (52.11%); 5712 in COG (31.10%); 9298 in Swiss-Prot (50.62%); 16,898 in eggNOG (92.00%); 12,958 in Pfam (70.55%); 7683 in GO (41.83%); and 12,527 in KOG (46.46%) (Table 4).

In addition, NR annotation revealed that 11,499 unigenes were matched to various species genomes such as *Zootermopsis nevadensis* (2111, 13.61%), *Daphnia pulex* (1046, 6.74%), *Stegodyphus mimosarum* (654, 4.22%), *Tribolium castaneum* (537, 3.46%), *Branchiostoma floridae* (514, 3.31%), *Saccoglossus kowalevskii* (458, 2.95%), *Capitella teleta* (351, 2.26%), *Lottia gigantea* (336, 2.17%), *Pediculus humanus* (332, 2.14%), *Strongylocentrotus purpuratus* (320, 2.06%) and others (8857, 57.08%) (Fig. 2).

3.3. Classification of transcriptome sequences

A total of 7683 unigenes were classified into three main categories on the basis of their functional annotation, including “biological

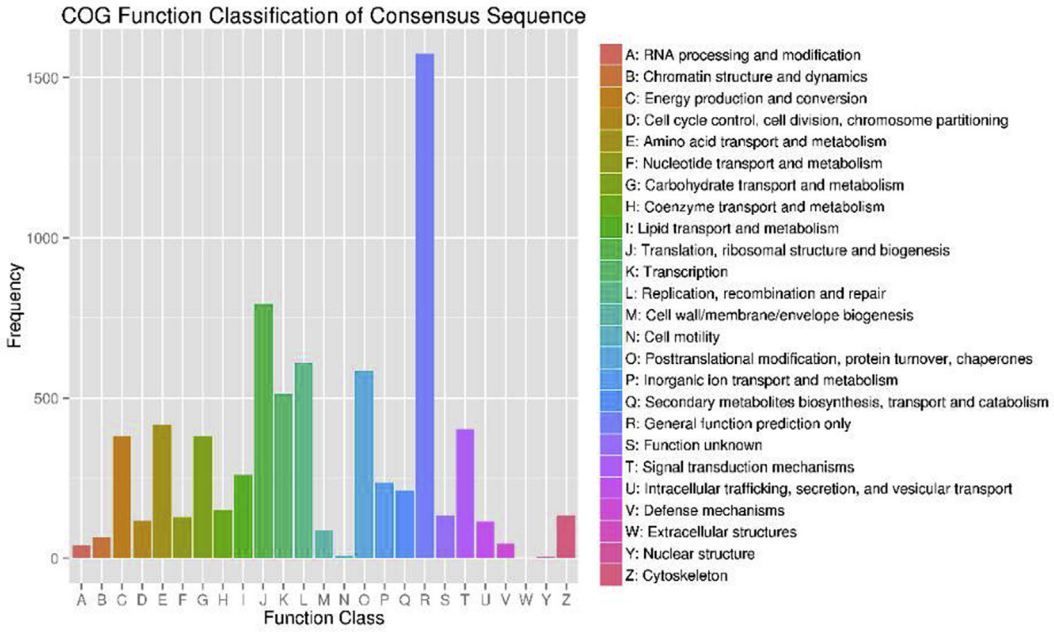

Fig. 4. COG function classification of consensus sequence. The X-axis represents names of 25 groups, the Y-axis corresponds to the number of genes in the group.

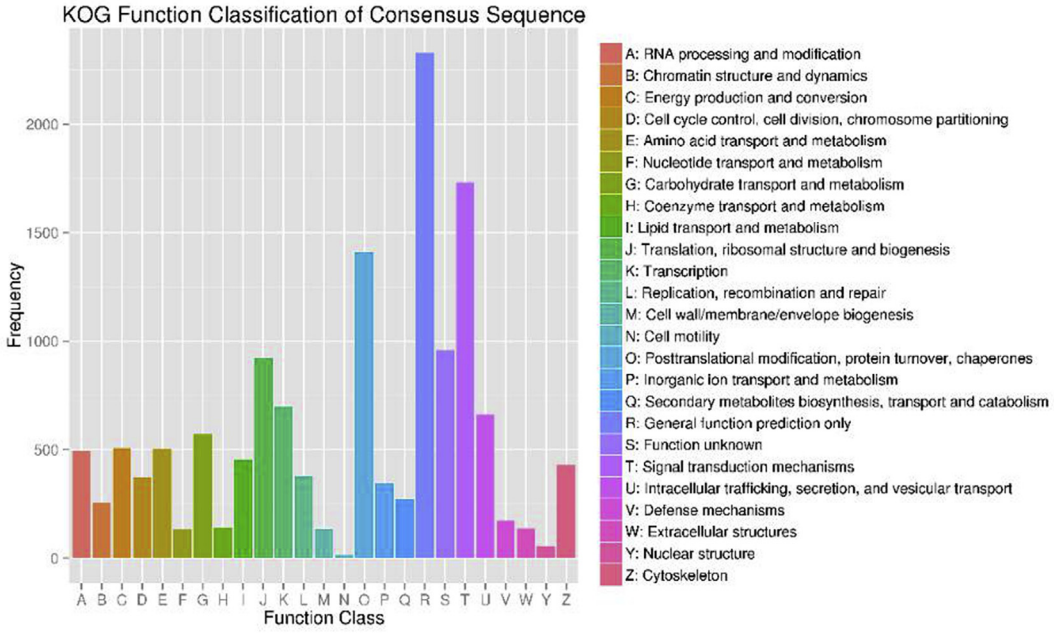

Fig. 5. KOG function classification of consensus sequence. The X-axis represents the names of the 26 groups, and the Y-axis corresponds to the percentage of the number of genes in the group accounting for the total number of annotated genes.

process" (BP), "cellular component" (CC), and "molecular function" (MF). Further, they were categorized 19, 17, and 15 subcategories in the biological process, cellular component and molecular function categories, respectively. Most of unigenes in the "biological process" category were involved in "cellular process" and "metabolic process", which included 3992 (21.57%) and 3893 (21.03%) unigenes, respectively. Within the "cellular component" category, a number of unigenes were assigned to "cell" (2570, 22.14%) and "cell part" (2568, 22.12%) subcategories. In the "molecular function" category, the most abundant groups were "catalytic activity" (4179, 43.28%) and "binding" (3785, 39.20%). Unigenes were assigned to the main GO categories as follows: 18,510 associated to BP, 11,608 to CC and 9655 to MF (Fig. 3 and Table 5).

In addition, a total of 5712 and 12,527 unigenes were classified into 25 categories in the COG and KOG database, respectively. Among these categories, "general function prediction only" is the largest group (Fig. 4 and Fig. 5).

3.4. Identification and analysis of DEGs

Among the identified unigenes, many genes were found to be differentially expressed after LPS challenge. Through the differential expression analysis, we identified a total of 2215 significant DEGs between the LPS-challenge and PBS control groups. As shown in volcano plot, of these unigenes, 669 were strongly upregulated and 1546 downregulated. In the volcano plot, the red pots represent significantly

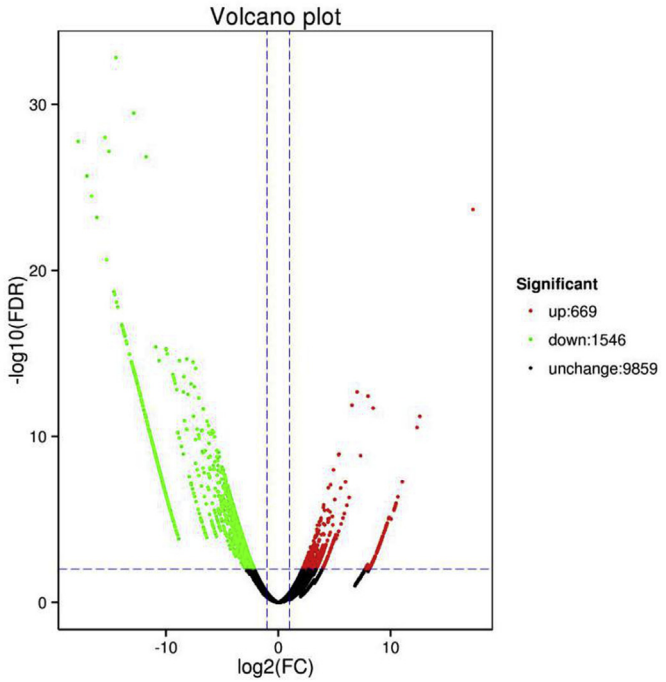

Fig. 6. Volcano plot of DEGs identified between LPS and PBS group. The red pots represent significantly up-regulated unigenes. The green pots represent significantly down-regulated unigenes. The black pots mean no significantly differential expression.

up-regulated unigenes, the green pots represent significantly down-regulated unigenes and the black pots mean no significantly differential expression (Fig. 6). The number of DEGs identified in different functional databases were: 536 in COG, 625 in GO, 657 in KEGG, 984 in KOG, 1251 in Pfam, 883 in Swiss-Prot, 1307 in eggNOG, and 1370 in NR (Table 6).

3.5. Identification and analysis of DEGs

All DEGs were categorized into three GO categories by topGO, including "biological process" (BP), "cellular component" (CC), and "molecular function" (MF), containing 18, 14, and 12 subcategories, respectively. Among the BP categories, the top three by frequency were "metabolic process", "cellular process" and "single-organism process" with 318, 264 and 232 DEGs, respectively. Moreover, the subcategory "immune system process" (9 DEGs) was closely related to immune response. Within the CC category, "cell" (182 DEGs), "cell part" (182 DEGs), and "organelle" (141 DEGs) were most abundant subcategories. Whereas the top clusters by frequency were "catalytic activity" (357 DEGs), "binding" (242 DEGs), and "structural molecule activity" (43 DEGs) in the MF category, (Fig. 3 and Table 5). Among these subcategories, "antioxidant activity" was associated with immune and antioxidant responses.

COG annotation revealed that a total of 724 DEGs could be classified into 25 categories. Of which, "general function prediction only (R)" (153, 21.13%) was the largest group, followed by "amino acid transport and metabolism (E)" (67, 6.25%) and "carbohydrate transport and metabolism (G)" (61, 8.43%). Eight DEGs (1.10%) were related to the "Defense mechanisms (V)". Additionally, the biological role of ten DEGs remained unknown (Fig. 7 and Table 7).

KEGG pathways were divided into four categories: "cellular processes", "environmental information processing", "genetic information processing", and "metabolism". The top 20 KEGG pathways and their term types are shown in Table. Among these pathways, "ribosome" was the largest group, which had 34 DEGs, followed by "lysosome" (29 DEGs), "carbon metabolism" (27 DEGs) and "biosynthesis of amino acids" (24 DEGs). In addition, within the top 20 KEGG pathways, four were related to "cellular processes" term type, with "lysosome" (29 DEGs) being the most abundant group. Four were associated with "genetic information processing" category, in which the largest group was "ribosome" (34 DEGs). Twelve were involved in "metabolism" category, which is the most common category, of which "carbon metabolism" (27 DEGs) was the biggest group (Table 8). The ribosome is the central player in cellular protein synthesis, polymerizing amino acids in the order dictated by the genetic information in the mRNA [44]. Ribosome composition (both RNA and protein) plays an important role in the regulation of cell physiology [45]. Lysosomes play key biological roles in innate immunity and various aspects of cell physiology, which are involved in the process of immune cells against pathogens [46]. They also participate in fundamental functions required for plasma membrane repair, signaling transduction and energy metabolism [47]. Amino acids have the potential effects on various physiological and immunological functions in animals [48].

3.6. qRT-PCR analysis of DEGs

To ensure the reliability of DEGs, we selected several immune-related genes for qRT-PCR, including Cofilin, Cysteine proteinase, HSP21, HSP70, Phospholipase D, Myeloid differentiation factor 88, Ras-related protein Ral-a, Serine/threonine protein kinase, TGF bata-inducible nuclear protein and tar RNA binding protein (Fig. 8). In comparison with the control group, most genes were upregulated and increased at least two-fold, which are consistent with those obtained by the transcriptome. Additionally, HSP70 expression was remarkably enhanced (15-fold) compared to PBS group. It suggests that HSP70 is the most strongly induced in response to various cellular stresses [49]. HSP70s play important roles in immune responses against bacterial infections to protect cells [50], participating in many important cellular processes including protein synthesis, translocation, assembly, and degradation [51]. Relatively speaking, HSP21 expression was not greatly increased, however upregulation was observed as reported in nervous tissue [52]. Protein kinases regulate the metabolic process, functions of nervous system, immune responses, and also playing pivotal roles in nearly every aspect of cell physiology [53]. RNA-binding proteins are critically important to the structure and interactions of the RNAs and play critical roles in their biogenesis, stability, function, transport and cellular localization [54], involving in the inflammation and immune processes. Accordingly, our study is reliable enough to perform further investigation.

3.7. Pathways related to immune response

The peroxisome pathway seems to be involved in immune responses (Fig. S1). Cara and his co-workers suggested that peroxisomes are required for immune responses for microbial infections [55]. We observed upregulation in the several peroxisome-associated genes such as peroxin-3 (PEX3), phytanoyl-CoA hydroxylase (PHYH), long-chain acyl-CoA synthetase (ACSL) and xanthine dehydrogenase/oxidase

Table 6
Number of DEGs in different function database.

DEG set	Annotated	COG	GO	KEGG	KOG	Pfam	Swiss-Prot	EggNOG	Nr
PBS vs LPS	1459	536	625	657	984	1251	883	1307	1370

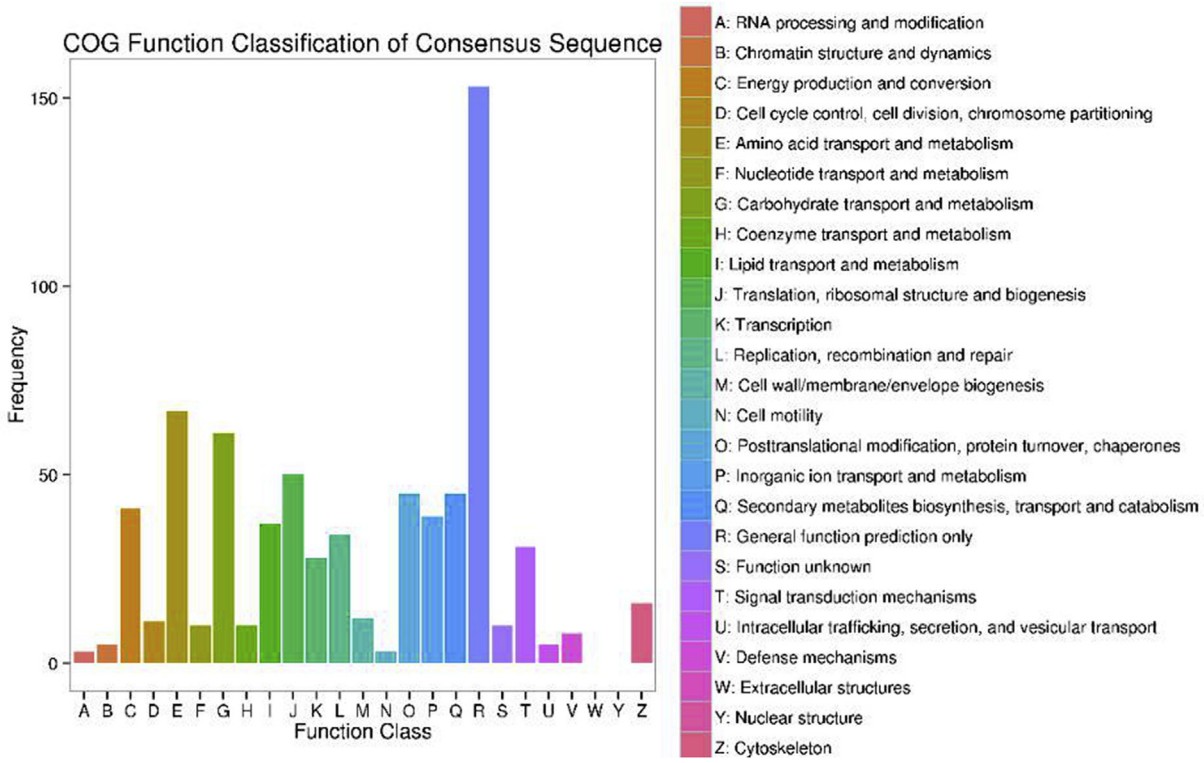

Fig. 7. Classification of the unigenes annotated in COG. The X-axis represents names of 25 groups, the Y-axis corresponds to the number of genes in the group.

Table 7
Classification table of the unigenes annotated in COG.

Class name	Abbreviation	Numbers	Percentage (%)
Translation, ribosomal structure and biogenesis	J	50	6.91
RNA processing and modification	A	3	0.41
Transcription	K	28	3.87
Replication, recombination and repair	L	34	4.70
Chromatin structure and dynamics	B	5	0.69
Cell cycle control, cell division, chromosome partitioning	D	11	1.52
Nuclear structure	Y	0	0
Defense mechanisms	V	8	1.10
Signal transduction mechanisms	T	31	4.28
Cell wall/membrane/envelope biogenesis	M	12	1.66
Cell motility	N	3	0.41
Cytoskeleton	Z	16	2.21
Extracellular structures	W	0	0
Intracellular trafficking, secretion, and vesicular transport	U	5	0.69
Posttranslational modification, protein turnover, chaperones	O	45	6.22
Energy production and conversion	C	41	5.66
Carbohydrate transport and metabolism	G	61	8.43
Amino acid transport and metabolism	E	67	9.25
Nucleotide transport and metabolism	F	10	1.38
Coenzyme transport and metabolism	H	10	1.38
Lipid transport and metabolism	I	37	5.11
Inorganic ion transport and metabolism	P	39	5.39
Secondary metabolites biosynthesis, transport and catebolism	Q	45	6.22
General function prediction only	R	153	21.13
Function unknown	S	10	1.38

(XDH). While some of the genes showed down regulation, including Peroxin-11B (PEX11), acyl-CoA oxidase (ACOX), bile acid-CoA: amino acid N-acyltransferase (BAAT) and so on. Peroxisomes are single membrane-bound organelle found in approximately all eukaryotic organisms [56]. They regulate many important metabolic pathways, including the β-oxidation of fatty acids, synthesis of ether glycerophospholipids and bile acids, the catabolism of some amino acids and polyamines and detoxification of reactive oxygen species [57]. PEX3 protein is believed to contain only one transmembrane domain and exposing the majority of its polypeptide chain into the cytosol [58]. The PEX3p is a peroxisomal integral membrane protein that controls maturation of preperoxisome biogenesis, whereas PEX3 involves in assembly of peroxisomal membrane [59]. PHYH catalyzes a key step in the fatty acid metabolism [60]. The α-oxidation pathway-associated enzymes are produced in a variety of organisms, indicating its importance in general detoxification mechanism [61]. ACSL belongs to the acyl-CoA synthetase (ACS) family, catalyzing free FA thioesterification to CoA [62]. ACSL proteins play important roles in lipid synthesis and

Table 8
Unigene number in the top 20 KEGG pathway.

Pathway	Term Type	All genes in pathway	DEGs in pathway
Ribosome	Genetic Information Processing	463	34
Lysosome	Cellular Processes	178	29
Carbon metabolism	Metabolism	198	27
Biosynthesis of amino acids	Metabolism	177	24
Phagosome	Cellular Processes	166	20
Oxidative phosphorylation	Metabolism	202	19
RNA transport	Genetic Information Processing	197	18
Glycolysis/gluconeogenesis	Metabolism	122	18
Protein processing in endoplasmic reticulum	Genetic Information Processing	245	14
Spliceosome	Genetic Information Processing	213	14
Peroxisome	Cellular Processes	113	13
Arginine and proline metabolism	Metabolism	74	12
Starch and sucrose metabolism	Metabolism	59	12
Glycerolipid metabolism	Metabolism	53	12
Endocytosis	Cellular Processes	178	11
Glutathione metabolism	Metabolism	79	11
Glycine, serine and threonine metabolism	Metabolism	45	11
Purine metabolism	Metabolism	196	10
Amino sugar and nucleotide sugar metabolism	Metabolism	63	10
Glyoxylate and dicarboxylate metabolism	Metabolism	63	10

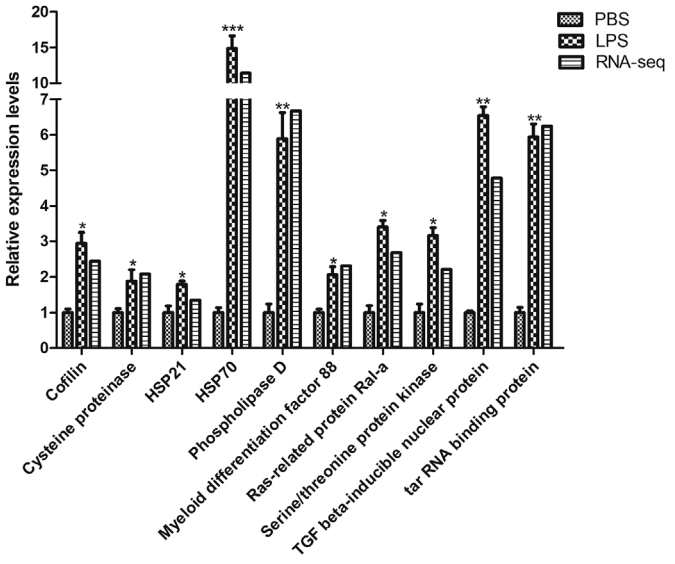

Fig. 8. Relative expression profiles of several genes involved in the immune response to the LPS challenge. The 18S rRNA gene was used as an internal reference. Gene expression levels in the control group were set as 1.0. Data are expressed as mean fold-change (mean ± standard error, n = 3) relative to the control group. The values were significantly different to the control at the same time point when marked with asterisks (*P < 0.05, **P < 0.01, ***P < 0.001).

storage, fatty acid catabolism, vectorial acylation, and synthesis of cutin and wax, and their activities are required for active fatty acids [63]. Xanthine oxidase is a versatile metalloflavoprotein enzyme, belonging to reactive oxygen species-generating oxidases, it catalyze the oxidative hydroxylation of hypoxanthine and xanthine to uric acid in purine catabolism, while simultaneously producing reactive oxygen species [64,65]. From the KEGG pathway analysis, we can get to know more about immune responses and metabolism of *P. clarkii* hepatopancreas against LPS injection.

The hepatopancreas and hemolymph are considered the vital tissues and organs of shrimp humoral immunity and cellular immunity. To date, many authors suggested that excessive production of ammonia can inhibit normal immune function of shrimp and the hepatopancreas involves in ammonia-stress responses of shrimp [66], suggesting that hepatopancreas is an important organ to study transcriptomic changes during ammonia treatment [67]. The crustacean hepatopancreas is the most important tissue and plays an important role in detoxification, organic metabolism and immune defense system, the study of *P. clarkii* under the stress of Cd [68] and Cr [69] also selected hepatopancreas as the target tissue. The present study may enrich the data of hepatopancreas with the method of high-throughput sequencing.

Recent studies on shrimp have shown that, some specific complex carbohydrates can induce the host to enhance their immunity and have immune activation characteristics, which are known as immunostimulants [70]. At present, microbial derivatives are one of the main immunostimulants such as LPS and PGN, which are widely used to study immune responses in aquatic animals. In crustaceans, immunostimulants activate phagocytes and improve their phagocytosis efficiency; stimulate the generation of antibacterial and lysozyme activity in hemolymph; activate prophenol oxidase system and produce recognition signals [71]. Sritunyalucksana et al. reported that antibacterial activity of black tiger prawn is enhanced after LPS treatment [72]. Though immunostimulants can effectively enhance the activity of immune factors, a large quantity of immunostimulants have been found to cause immunosuppression in host.

4. Conclusion

In conclusion, in this study, we analyzed hepatopancreas transcriptome of *P. clarkii* after LPS and PBS injection. A total of 55,107 unigenes were identified, which were annotated using different functional databases, including NR, Swiss-Prot, GO, COG, KOG, eggNOG, and KEGG. Among the identified DEGs (2215), 669 were found to be up-regulated genes and 1546 down-regulated genes. This study shed a light on the transcriptome of *P. clarkii* and also improves our knowledge regarding the immune-related genes and immune responses of *P. clarkii* to LPS challenge. At the same time, it also provides new insight into understanding *P. clarkii* immune defense mechanism against bacterial infections, contributing to further study.

Declaration of competing interest

The authors declare no competing interests.

Acknowledgements

This work was supported by the Natural Science Foundation of Jiangsu Province (BK20160444), the National Natural Science

Foundation of China (31600740 and 31640074), the China Postdoctoral Science Foundation (2018M642105), the Jiangsu Agricultural Science and Technology Innovation Fund (CX(18)3027), the Research Start-up Fund of Wenzhou Medical University (QTJ16021), the Scientific and Technological Innovation Special Project for Seed and Seedling of Wenzhou Science & Technology Bureau (Z20170014), the Opening Project of Zhejiang Provincial Top Key Discipline of Pharmaceutical Sciences (201721), the 16th Six Talents Peak Project of Jiangsu Province (NY-126), the Jiangsu Key Laboratory for Bioresources of Saline Soils (JKLBS2017010), and sponsored by Qing Lan Project of Jiangsu Province.

Appendix A. Supplementary data

Supplementary data to this article can be found online at https://doi.org/10.1016/j.fsi.2019.09.072

References

[1] E. Tricarico, S. Bertocchi, S. Brusconi, E. Casalone, F. Gherardi, G. Giorgi, G. Mastromei, G. Parisi, Depuration of microcystin-LR from the red swamp crayfish *Procambarus clarkii* with assessment of its food quality, Aquaculture 285 (2008) 90–95.

[2] O. Cremades, E. Ponce, R. Corpas, J.F. Gutiérrez, M. Jover, M.C. Alvarez-Ossorio, J. Parrado, J. Bautista, Processing of crawfish (*Procambarus clarkii*) for the preparation of carotenoproteins and chitin, J. Agric. Food Chem. 49 (2001) 5468–5472.

[3] C.F. Yue, T.T. Wang, Y.F. Wang, Y. Peng, Effect of combined photoperiod, water calcium concentration and PH on survival, growth, and moulting of juvenile crayfish (*Procambarus clarkii*) cultured under laboratory conditions, Aquacult. Res. 40 (2009) 1243–1250.

[4] X.M. Hua, C. Shui, Y.D. He, S.H. Xing, N. Yu, Z.Y. Zhu, C.Y. Zhao, Effects of different feed stimulants on freshwater crayfish (*Procambarus clarkii*), fed diets with or without partial replacement of fish meal by biofeed, Aquacult. Nutr. 21 (2015) 113–120.

[5] W.R. McClain, Growth of crawfish *Procambarus clarkii* as a function of density and food resources, J. World Aquac. Soc. 26 (1995) 24–28.

[6] Z.Q. Du, Y.H. Jin, D.M. Ren, In-depth comparative transcriptome analysis of intestines of red swamp crayfish, *Procambarus clarkii*, infected with WSSV, Sci. Rep. 6 (2016) 26780.

[7] K. Wang, X.L. Shen, J.S. Jia, X.D. Yu, J. Du, S.H. Lin, Z.Q. Du, High-throughput sequencing analysis of microRNAs in gills of red swamp crayfish, *Procambarus clarkii* infected with white spot syndrome virus, Fish Shellfish Immunol. 83 (2018) 18–25.

[8] P. Amparyup, W. Charoensapsri, A. Tassanakajon, Prophenoloxidase system and its role in shrimp immune responses against major pathogens, Fish Shellfish Immunol. 34 (2013) 990–1001.

[9] H.H. Du, W.F. Li, Z.R. Xu, Z.S. Kil, Effect of hyperthermia on the replication of white spot syndrome virus (WSSV) in *Procambarus clarkii*, Dis. Aquat. Org. 71 (2006) 175–178.

[10] B.K. Chen, Z. Dong, D.P. Liu, Y.B. Yan, N.Y. Pang, Y.Y. Nian, D.C. Yan, Iinfectious hypodermal and haematopoietic necrosis virus (IHHNV) infection in freshwater crayfish *Procambarus clarkii*, Aquaculture 477 (2017) 76–79.

[11] D.D. Chen, X.L. Meng, J.P. Xu, J.Y. Yu, M.X. Meng, J. Wang, PcTL, a novel C-type lectin from *Procambarus clarkii*, is involved in the innate defense against *Vibrio alginolyticus* and WSSV, Dev. Comp. Immunol. 39 (2013) 255–264.

[12] Z.F. Ding, J. Du, J.T. Ou, W.J. Li, T. Wu, Y.J. Xiu, Q.G. Meng, Q. Ren, W. Gu, H. Xue, J.Q. Tang, W. Wang, Classification of circulating hemocytes from the red swamp crayfish *Procambarus clarkii* and their susceptibility to the novel pathogen *Spiroplasma eriocheiris* in vitro, Aquaculture 356–357 (2012) 371–380.

[13] L.S. Dai, S.H. Chu, X.M. Yu, Y.Y. Li, A role of cathepsin L gene in innate immune response of crayfish (*Procambarus clarkii*), Fish Shellfish Immunol. 71 (2017) 246–254.

[14] J.T. Li, J. Li, P. Chen, P. Liu, Y.Y. He, Transcriptome analysis of eyestalk and hemocytes in the ridgetail white prawn *Exopalaemon carinicauda*: assembly, annotation and marker discovery, Mol. Biol. Rep. 42 (2015) 135–147.

[15] L.F. Fan, A.L. Wang, Y.T. Miao, S.A. Liao, C.X. Ye, Q.C. Lin, Comparative proteomic identification of the hepatopancreas response to cold stress in white shrimp, *Litopenaeus vannamei*, Aquaculture 454 (2016) 27–34.

[16] J. Du, H.X. Zhu, P. Liu, J. Chen, Y.J. Xiu, W. Yao, T. Wu, Q. Ren, Q.G. Meng, W. Gu, W. Wang, Immune responses and gene expression in hepatopancreas from *Macrobrachium rosenbergii* challenged by a novel pathogen spiroplasma MR-1008, Fish Shellfish Immunol. 34 (2013) 315–323.

[17] L.S. Dai, M.N. Abbas, S. Kausar, Y. Zhou, Transcriptome analysis of hepatopancraes of *Procambarus clarkii* challenged with polyriboinosinic polyribocytidylic acid (poly I: C), Fish Shellfish Immunol. 71 (2017) 144–150.

[18] H. Yang, X.J. Gao, X.X. Li, H.H. Zhang, N. Chen, Y.Y. Zhang, X.D. Liu, X.J. Zhang, Comparative transcriptome analysis of red swamp crayfish (*Procambarus clarkia*) hepatopancreas in response to WSSV and *Aeromonas hydrophila* infection, Fish Shellfish Immunol. 83 (2018) 397–405.

[19] A.O. Antwi, D.D. Obiri, N. Osafo, A.D. Forkuo, L.B. Essel, Stigmasterol inhibits lipopolysaccharide-induced innate immune responses in murine models, Int. Immunopharmacol. 53 (2017) 105–113.

[20] X.Q. Wei, K. Lan, Activation and counteraction of antiviral innate immunity by KSHV: an update, Sci. Bull. 63 (2018) 1223–1234.

[21] V.P. Sampath, Bacterial endotoxin-lipopolysaccharide; structure, function and its role in immunity in vertebrates and invertebrates, Agr. Nat. Resour. 52 (2018) 115–120.

[22] Y.H. Chih, S.Y. Wang, B.S. Yip, K.T. Cheng, S.Y. Hsu, C.L. Wu, H.Y. Yu, J.W. Cheng, Dependence on size and shape of non-nature amino acids in the enhancement of lipopolysaccharide (LPS) neutralizing activities of antimicrobial peptides, J. Colloid Interface Sci. 533 (2019) 492–502.

[23] H. Han, A novel feature selection for RNA-seq analysis, Comput. Biol. Chem. 71 (2017) 245–257.

[24] P. Wang, F.F. Wang, J. Yang, De novo assembly and analysis of the *Pugionium cornutum* (L.) Gaertn. transcriptome and identification of genes involved in the drought response, Gene 626 (2017) 290–297.

[25] J.J. Lv, P. Liu, Y. Wang, B.Q. Gao, P. Chen, J. Li, Transcriptome analysis of *Portunus trituberculatus* in response to salinity stress provides insights into the molecular basis of osmoregulation, PLoS One 8 (2013) e82155.

[26] B.J. Haas, A. Papanicolaou, M. Yassour, M. Grabherr, P.D. Blood, J. Bowden, M.B. Couger, D. Eccles, B. Li, M. Lieber, M.D. Macmanes, M. Ott, J. Orvis, N. Pochet, F. Strozzi, N. Weeks, R. Westerman, T. William, C.N. Dewey, R. Henschel, R.D. Leduc, N. Friedman, A. Regev, De novo transcrip sequence reconstruction from RNA-seq using the Trinity platform for reference generation and analysis, Nat. Protoc. 8 (2013) 1494–1512.

[27] K. Yu, T. Zhang, Construction of customized sub-databases from NCBI-nr database for rapid annotation of huge metagenomic datasets using a combined BLAST and MEGAN approach, PLoS One 8 (2013) e59831.

[28] J.H. Zuo, Y.X. Wang, B.Z. Zhu, Y.B. Luo, Q. Wang, L.P. Gao, sRNAome and transcriptome analysis provide insight into chilling response of cowpea pods, Gene 671 (2018) 142–151.

[29] A. Bairoch, R. Apweiler, The Swiss-prot protein sequence database and its supplement TrEMBL in 2000, Nucleic Acids Res. 28 (2000) 45–48.

[30] M. Kanehisa, S. Goto, M. Furumichi, M. Tanabe, M. Hirakawa, KEGG for representation and analysis of molecular networks involving diseases and drugs, Nucleic Acids Res. 38 (2010) 355–360.

[31] J.A. Blake, M.A. Harris, The Gene Ontology (GO) project: structured vocabularies for molecular biology and their application to genome and expression analysis, Curr. Protoc. Bioinformatics 23 (2008) 721–729.

[32] R.L. Tatusov, M.Y. Galperin, D.A. Natale, E.V. Koonin, The COG database: a tool for genome-scale analysis of protein functions and evolution, Nucleic Acids Res. 28 (2000) 33–36.

[33] F. Yin, Q.X. Gao, B.J. Tang, P. Sun, K.H. Han, W.Q. Huang, Transcriptome and analysis on the complement and coagulation cascades pathway of large yellow croaker (*Larimichthys crocea*) to ciliate ectoparasite *Cryptocaryon irritans* infection, Fish Shellfish Immunol. 50 (2016) 127–141.

[34] L.W. Liu, Y.Z. Sui, W.B. Zhu, A. Guo, K.D. Xu, Y.D. Zhou, In-depth transcriptome analysis of *Larimichthys polyactis*, de novo assembly, functional annotation, Mar. Genomics 33 (2017) 27–29.

[35] F.R. Lou, T.Y. Yang, Z.Q. Han, T.X. Gao, Transcriptome analysis for identification of candidate genes related to sex determination and growth in *Charybdis japonica*, Gene 677 (2018) 10–16.

[36] C.N. Dewey, L. Bo, RSEM: accurate transcript quantification from RNA-Seq data with or without a reference genome, BMC Bioinf. 12 (2011) 323.

[37] F.J. Jiang, X. Yue, H.X. Wang, B.Z. Liu, Transcriptome profiles of the clam *Meretrix petechialis* hepatopancreas in response to *Vibrio* infection, Fish Shellfish Immunol. 62 (2017) 175–183.

[38] J. Yang, Y.C. Hu, K. Xiao, X.Q. Liu, C. Tan, B.Z. Wang, H.J. Du, Transcriptome profiling reveals candidate cleft palate-related genes in cultured Chinese sturgeons (*Acipenser sinensis*), Gene 666 (2018) 1–8.

[39] X.R. Chen, Prediction of optimal gene functions for osteosarcoma using gene ontology and microarray profiles, J. Bone Oncol. 7 (2017) 18–22.

[40] R.C. Lovering, E.C. Dimmer, P.J. Talmud, Improvements to cardiovascular gene ontology, Atherosclerosis 205 (2009) 9–14.

[41] V. Ponesakki, S. Paul, D.K.S. Mani, V. Rajendiran, P. Kanniah, S. Sivasubramaniam, Annotation of nerve cord transcriptome in earthworm *Eisenia fetida*, Genom, Data 14 (2017) 91–105.

[42] H. Jiang, Z. Qian, W. Lu, H. Ding, H. Yu, H. Wang, J. Li, Identification and characterization of reference genes for normalizing expression data from red swamp crawfish *Procambarus clarkii*, Int. J. Mol. Sci. 16 (2015) 21591–21605.

[43] L. Wu, Y. Zhou, M.N. Abbas, S. Kausar, Q. Chen, C.X. Jiang, L.S. Dai, Molecular structure and functional characterization of the peroxiredoxin 5 in *Procambarus clarkii* following LPS and Poly I:C challenge, Fish Shellfish Immunol. 71 (2017) 28–34.

[44] C.M. Kaiser, K.X. Liu, Folding up and moving on – nascent protein folding on the ribosome, J. Mol. Biol. 430 (2018) 4580–4591.

[45] J.E. Gerst, Pimp my ribosome: ribosomal protein paralogs specify translational control, Trends Genet. 34 (2018) 832–845.

[46] L.A. Huber, D. Teis, Lysosomal signaling in control of degradation pathways, Curr. Opin. Cell Biol. 39 (2016) 8–14.

[47] A. Reddy, E.V. Caler, N.W. Andrews, Plasma membrane repair is mediated by Ca (2+)-regulated exocytosis of lysosomes, Cell 106 (2001) 157–169.

[48] R.T. Pereira, P.V. Rosa, D.M. Gatlin, Glutamine and arginine in diets for Nile tilapia: effects on growth, innate immune responses, plasma amino acid profiles and whole-body composition, Aquaculture 473 (2017) 135–144.

[49] L. Li, L.L. Wang, J.Y. He, Z.J. Chang, Expression of Hsp70 reveals significant differences between fin regeneration and inflammation in *Paramisgurnus dabryanus*, Fish Shellfish Immunol. 64 (2017) 352–356.
[50] N. Chen, X.L. Wan, C.X. Huang, W.M. Wang, H. Liu, H.L. Wang, Study on the immune response to recombinant Hsp70 protein from *Megalobrama amblycephala*, Immunobiology 219 (2014) 850–858.
[51] W. Dang, Y.H. Hu, M. Zhang, L. Su, Identification and molecular analysis of a stress-inducible Hsp70 from *Sciaenops ocellatus*, Fish Shellfish Immunol. 29 (2010) 600–607.
[52] P.Y. Huang, S.T. Kang, W.Y. Chen, T.C. Hsu, C.F. Lo, K.F. Liu, L.L. Chen, Identification of the small heat shock protein, HSP21, of shrimp *Penaeus monodon* and the gene expression of HSP21 is inactivated after white spot syndrome virus (WSSV) infection, Fish Shellfish Immunol. 25 (2008) 250–257.
[53] R.R. Jr, Targeting oncogenic Raf protein-serine/threonine kinases in human cancers, Pharmacol. Res. 135 (2018) 239–258.
[54] T. Glisovic, J.L. Bachorik, J. Yong, G. Dreyfuss, RNA-binding proteins and post-transcriptional gene regulation, FEBS Lett. 582 (2008) 1977–1986.
[55] F.D. Cara, A. Sheshachalam, N.E. Braverman, R.A. Rachubinski, A.J. Simmonds, Peroxisome-mediated metabolism is required for immune response to microbial infection, Immunity 47 (2017) 93–106.
[56] A. Schluter, S. Fourcade, R. Ripp, J.L. Mandel, O. Poch, A. Pujol, The evolutionary origin of peroxisomes: an ER-peroxisome connection, Mol. Biol. Evol. 23 (2006) 838–845.
[57] R.J. Wanders, H.R. Waterham, Biochemistry of mammalian peroxisomes revisited, Annu. Rev. Biochem. 75 (2006) 295–332.
[58] M.P. Pinto, C.P. Grou, M. Fransen, C. Sá-Miranda, J.E. Azevedo, The cytosolic domain of PEX3, a protein involved in the biogenesis of peroxisomes, binds membrane lipids, Biochim. Biophys. Acta Mol. Cell Res. 1793 (2009) 1669–1675.
[59] S. Matsui, M. Funahashi, A. Honda, N. Shimozawa, Newly identified milder phenotype of peroxisome biogenesis disorder caused by mutated PEX3 gene, Brain Dev. 35 (2013) 842–848.
[60] Z.H. Zhang, G.T. Kochan, S.S. Ng, K.L. Kavanagh, U. Oppermann, C.J. Schofield, M.A. Mcdonough, Crystal structure of PHYHD1A, a 2OG oxygenase related to phytanoyl-CoA hydroxylase, Biochem. Biophys. Res. Commun. 408 (2011) 553–558.
[61] M. Mukherji, N.J. Kershaw, C.J. Schofield, A.S. Wierzbicki, M.D. Lloyd, Utilization of sterol carrier protein-2 by phytanoyl-CoA 2-hydroxylase in the peroxisomal α oxidation of phytanic acid, Chem. Biol. 9 (2002) 597–605.
[62] Y.S. Zheng, H. Chen, Y.J. Yuan, Y.F. Wang, L.Z. Chen, X.X. Liu, D.D. Li, Cloning and functional characterization of long-chain acyl-CoA synthetase 1 from the mesocarp of African oil palm (*Elaeis guineensis*, Jacq.), Ind. Crops Prod. 122 (2018) 252–260.
[63] C.L. Zhang, K. Mao, L.J. Zhou, G.L. Wang, Y.L. Zhang, Y.Y. Li, Y.J. Hao, Genome-wide identification and characterization of apple long-chain acyl-CoA synthetases and expression analysis under different stresses, Plant Physiol. Biochem. 132 (2018) 320–332.
[64] A. Šmelcerović, K. Tomović, Ž. Šmelcerović, Ž. Petronijević, G. Kocić, T. Tomašič, Ž. Jakopin, M. Anderluh, Xanthine oxidase inhibitors beyond allopurinol and febuxostat; an overview and selection of potential leads based on *in silico* calculated physico-chemical properties, predicted pharmacokinetics and toxicity, Eur. J. Med. Chem. 135 (2017) 491–516.
[65] J. Čejková, J. Labsky, J. Vacík, Reactive oxygen species (ROS) generated by xanthine oxidase in the corneal epithelium and their potential participation in the damage of the corneal epithelium after prolonged use of contact lenses in rabbits, Acta Histochem. 100 (1998) 171–184.
[66] X. Lu, J. Kong, S. Luan, P. Dai, X.H. Meng, B.X. Cao, K. Luo, Transcriptome analysis of the hepatopancreas in the Pacific white shrimp (*Litopenaeus vannamei*) under acute ammonia stress, PLoS One 11 (2016) e0164396.
[67] Y.D. Li, F.L. Zhou, J.H. Huang, L.S. Yang, S. Jiang, Q.B. Yang, J.G. He, S.G. Jiang, Transcriptome reveals involvement of immune defense, oxidative imbalance, and apoptosis in ammonia-stress response of the black tiger shrimp (*Penaeus monodon*), Fish Shellfish Immunol. 83 (2018) 162–170.
[68] Y. Zhang, Z.Y. Li, S. Kholodkevich, A. Sharov, Y.J. Feng, N.Q. Ren, K. Sun, Cadmium-induced oxidative stress, histopathology, and transcriptome changes in the hepatopancreas of freshwater crayfish (*Procambarus clarkii*), Sci. Total Environ. 666 (2019) 944–955.
[69] X. Meng, L. Hong, T.T. Yang, Y. Liu, T. Jiao, X.H. Chu, D.Z. Zhang, J.L. Wang, B.P. Tang, Q.N. Liu, W.W. Zhang, W.F. He, Transcriptome-wide identification of differentially expressed genes in *Procambarus clarkii* in response to chromium challenge, Fish Shellfish Immunol. 87 (2019) 43–50.
[70] X.H. Wang, J. Huang, X.L. Song, The application of immunostimulants-Peptidoglycan to the culture of shrimp, Mar. Fish. Res. 24 (2003) 70–75.
[71] J. Zhou, J. Huang, X.L. Song, Applications of immunostimulants in aquaculture, Mar. Fish. Res. 24 (2003) 70–79.
[72] K. Sritunyalucksana, P. Sithisam, B. Withayachumnarnkul, T.W. Flegel, Activation of prophenoloxidase, agglutinin and antibacterial activity in haemolymph of the black tiger prawn, *Penaeus monodon*, by immunostimulants, Fish Shellfish Immunol. 9 (1999) 21–30.